Electro-lattice actuator: a compliant high-contractile active lattice structure

OPEN ACCESS
IOP Publishing
Smart Materials and Structures
Smart Mater. Struct. **30** (2021) 125034 (9pp)
https://doi.org/10.1088/1361-665X/ac2ba9

Electro-lattice actuator: a compliant high-contractile active lattice structure

Sam Hoh[1,2], **Tim Helps**[1,2], **Richard Suphapol Diteesawat**[1,2,*], **Majid Taghavi**[1,2] **and Jonathan Rossiter**[1,2,*]

[1] Department of Engineering Mathematics, University of Bristol, Bristol BS8 1UB, United Kingdom
[2] Bristol Robotics Laboratory, Bristol BS16 1QY, United Kingdom

E-mail: jonathan.rossiter@bristol.ac.uk

Received 4 August 2021, revised 22 September 2021
Accepted for publication 29 September 2021
Published 15 November 2021

Abstract

Electro-ribbon actuators are high-performance electrically-driven artificial muscles with high flexibility, low mass, low power consumption, high contraction, and high force-to-weight ratio. They show great promise for driving the deployment of compact folding structures. This article presents the electro-lattice actuator (ELA), a compliant, three-dimensional, free-standing lattice structure that uses this phenomenon to contract to a flat sheet upon the application of a potential difference. The ELA was designed in the form of multiple interconnected buckled structures and fabricated using polyvinyl chloride sheets and tape and copper electrodes. The ELA structure was pre-set into an open-cell configuration by annealing in an oven. Isometric testing at varying compressions showed that the tensile stress of the proposed lattice actuator reaches a maximum of 184 Pa (a 472 Pa change in tensile stress compared with its unactuated state). A cuboid shaped ELA (13.6 cm length $\times$ 10.0 cm width $\times$ 5.4 cm height) achieved a contraction of 92.6% and a contraction rate of 35.6% s^{-1}. The novel ELA opens up the use of electro-ribbon actuation to more complex and more effective 3D actuating and deploying structures.

Supplementary material for this article is available online

Keywords: electro-ribbon actuator, electro-lattice actuator, lattice, contraction, soft actuator, zipping actuator

(Some figures may appear in colour only in the online journal)

1. Introduction

Recent developments in the field of robotics have shown an increased interest in soft, compliant robots that are able to easily adapt to their environment, leading to more robust and adaptive robots [1, 2]. To drive such robots, electrostatic actuators have been explored as a promising solution because they show quick response, are lightweight, have a small form factor, are readily scalable, and have the potential to generate extremely large forces [3]. Electrostatic actuators operate using electricity, a convenient and high energy-density power source compared with the fluidic reservoirs or compressors needed for pneumatically or hydraulically driven soft actuators. They exploit the strong electrostatic attraction force generated by two oppositely charged electrodes and employ an insulating medium between them to prevent electric breakdown.

Electrostatic actuators are commonly found in micro-electromechanical systems [4], however these actuators are highly limited in deflection due to the need for small electrode separations [5]. Further work has been undertaken to scale electrostatic actuators to macro-scale structures with larger deflections, leading to various soft actuators such as

* Authors to whom any correspondence should be addressed.

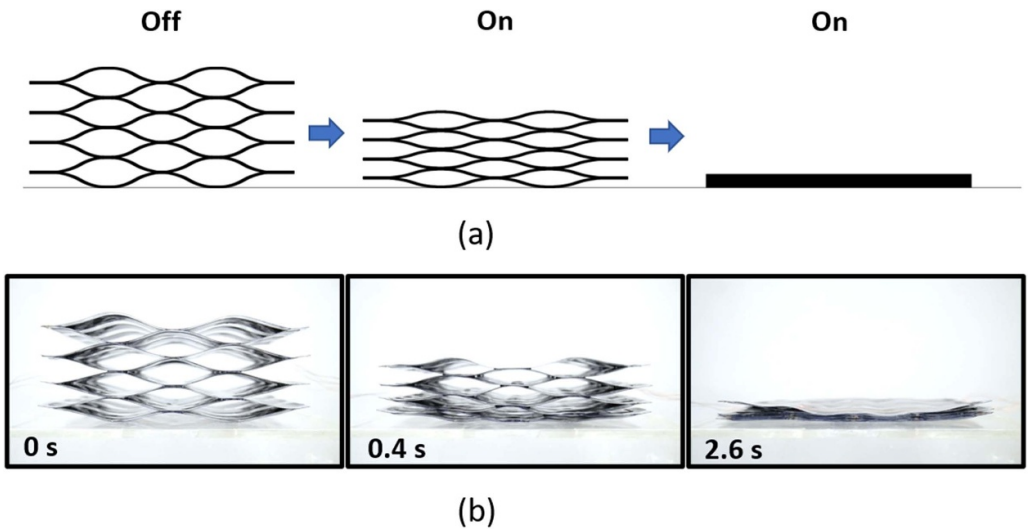

Figure 1. Representation of (a) the expected actuation behaviour of the ELA, where the 1st image shows the structure at rest, followed by contraction when the potential difference is applied. (b) The 3D cuboid ELA in action, showing full contraction from approximately 54 mm height to flat in approximately 2.6 s.

dielectric elastomer actuators [6], hydraulically amplified self-healing electrostatic actuators [7] and electro-ribbon actuators (ERAs) [8]. These actuators use a high-permittivity dielectric between the electrodes, which amplifies contractive electrostatic stresses. These stresses are coupled to the Maxwell stress, $P = \varepsilon E^2$, where ε is the permittivity of the dielectric, and E is the strength of the electric field [9]. Additionally, the use of a high-breakdown strength liquid dielectric in the ERAs ensures higher electric fields can be sustained, thereby increasing the contraction force between the electrodes by a factor of $\left(\frac{E_{\text{breakdown,liquid}}}{E_{\text{breakdown,air}}}\right)^2$ [8].

The ERA is an electrostatic dielectric zipping actuator that operates on the dielectrophoretic liquid zipping (DLZ) principle [8]. In particular, the ERA only requires the use of a small bead of liquid dielectric to achieve large strokes, significantly reducing the mass and volume of the actuator as compared to fully submerged or encapsulated devices. The ERA consists of two electrodes which are mechanically joined together to create a 'hinge' and at which a single droplet of liquid dielectric is placed. The dielectrophoretic forces generated by the electric field serve to hold the high-permittivity dielectric liquid in place at the hinge. As the actuator contracts, it moves the liquid dielectric along the actuator resulting in a 'zipping' motion and a continuous amplification of electrostatic force. This greatly reduces the weight and bulk of the actuator while still reaping the benefits of the force-amplifying liquid dielectric. The contractive force F generated at the zipping hinge can be approximated as,

$$F = \frac{\frac{1}{2}\varepsilon_0\varepsilon_{\text{medium}}AV^2}{\left(\frac{\varepsilon_{\text{medium}}}{\varepsilon_{\text{insulator}}}t_{\text{insulator}} + t_{\text{medium}}\right)^2} \quad (1)$$

where ε_0, $\varepsilon_{\text{medium}}$, and $\varepsilon_{\text{insulator}}$ are the permittivity of free space, the medium (in this case, the liquid dielectric) and the insulator, respectively, A is the area of the electrode, V is the applied voltage, and $t_{\text{insulator}}$ and t_{medium} are the thicknesses of the insulator and the medium, respectively [8].

Among the most exciting properties of the ERA are low weight, low power consumption, high contraction (up to 99.8% [8]), self-locking [10], self-sensing capabilities [11] and controllability [12]. ERA, and in a broader context, the DLZ actuation principle, present a potential candidate for developing future soft robotic technologies such as robotic origami [8] and compliant pumps [13]. In this paper, we extend this fundamental concept to design the electro-lattice actuator (ELA), a compliant, 3D free-standing, open-celled structure that is capable of contracting down to extremely low thickness (figure 1). The ELA also exhibits attractive spring-like behaviour which can be exploited to create lightweight, tuneable, and compliant actuators and variable stiffness components.

2. Methods and manufacturing

2.1. ELA manufacture

To create free-standing lattice structures, we first develop new methods for creating pre-bent ERAs. The most basic ERAs consist of two oppositely charged electrodes which are joined at both ends to create the hinges from which the zipping actuation can begin. Early experiments used a variety of flexible insulating and conducting materials, including steel and electrical polyvinyl chloride (PVC) tape, paper and pencil, and polyimide [8]. Recent experiments have used insulated copper tape electrodes mounted on PVC sheets which provide actuator stiffness [13]. Extending this configuration, two identical sheets can then be heat-sealed together to form a zipping structure without the use of clips, which unnecessarily increase actuator thickness (figure 2(a)).

An additional benefit of using the PVC sheet is that it can be annealed and reshaped easily, which allows it to be conveniently pre-formed into an open shape using a mould. Typical

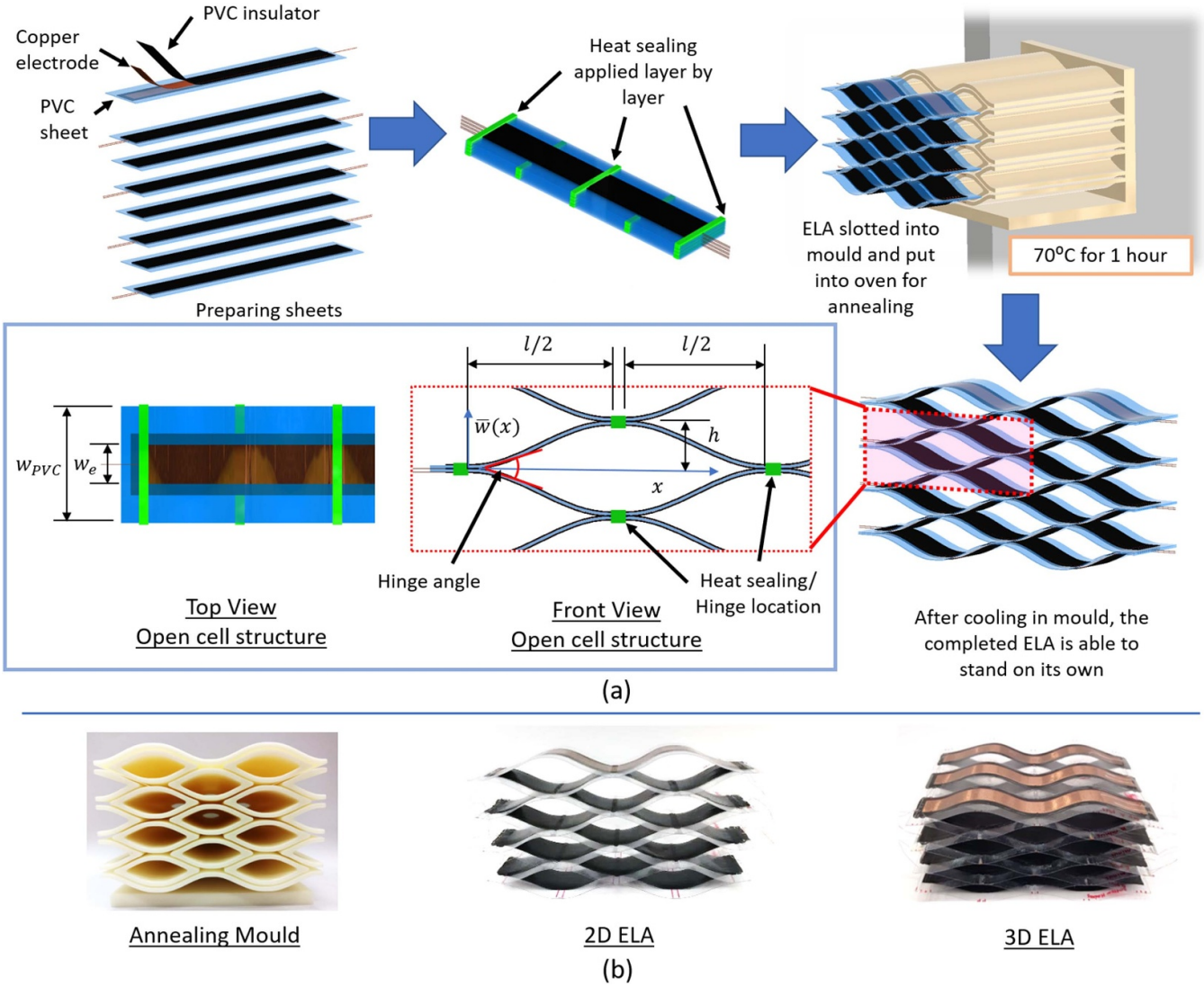

Figure 2. (a) Manufacturing method for ELAs. Dimensions of the open cell structure are determined before designing and preparing the moulds and materials, as shown in the inset. The individual sheets of the ELA are prepared by attaching the electrodes and insulators, after which the sheets are heat sealed together to create the hinges. The ELA is then slotted into the mould and placed in the oven at 70 °C until the ELA relaxes into the shape of the mould. The mould is taken out of the oven and left to cool at room temperature before the ELA is removed. The resulting structure has open cells and is primed for actuation. (b) From the left, the 3D printed mould, the basic 2D ELA, and the cuboid-shaped 3D ELA.

ERAs require pre-loading prior to actuation, since the ERA is, in its simplest form, a contracting actuator. By creating pre-bent ERAs, the need for pre-loading is removed, allowing for the development of free-standing devices.

To create an ELA, we first considered the shape of the open cell required. The shape of the open cell was designed so that it follows the curve of the first buckling mode of a beam. This shape follows the curve that is created during pre-loading of conventional ERAs and provides a stable configuration with minimum elastic energy [14].

If we consider the open cell to consist of two beams in the first buckling mode and connected at its ends, the curve equation is,

$$\bar{w}(x) = \frac{h}{2}\left[1 - \cos\left(2\pi\frac{x}{l}\right)\right] \tag{2}$$

where $\bar{w}(x)$ is the distance of each beam from the straight line connecting both ends, h is the apex height of the beam, x is the distance along the beam and l is the span of the beam, as illustrated in figure 2(a) inset.

Different cell shapes and patterns of the ELA can be widely fabricated; however, small hinge angles are consistently required for zipping initialisation. This is because a large hinge angle increases the distance between two insulated electrodes and thus decreases generated electrostatic force for structure contraction. Therefore, for the selected design following equation (2), it is important to choose the values of h and l such that the hinge angle is not too large. Electrostatic force is inversely proportional to the distance between the electrodes and therefore a large hinge angle makes it difficult for the actuator to initialise zipping. On the other hand, the width of the PVC sheet, w_{PVC}, and the thickness of the PVC sheet,

Table 1. Key dimensions of lattice actuator.

Parameter	Value (mm)
Apex height of beam, h	8.5
Span of beam, l	54.0
Width of PVC strip, w_{PVC}	36.0
Thickness of PVC, t_{PVC}	0.15
Width of electrode, w_e	12.0

t_{PVC}, affect the structural stiffness of the ELA and the generated force that is needed to contract the ELA. The width of the electrode, w_e, determines the amount of electrostatic force generated as described by equation (1). For this study, the values of these dimensions used to build the ELA are given in table 1. These were established based upon preliminary tests.

Once the dimensions were defined, the mould for holding the lattice open during annealing was designed and 3D-printed in ABS (ABS-M30 Filament, Stratasys, United States). The same parameters were also used to prepare the materials for the actuator. As shown in figure 2(a) inset, space needs to be allocated between half-beam sections for heat sealing. The dimensions of the mould and the prepared materials depend on the dimensions of the ELA lattice that is to be built.

First, the PVC sheets (A4 Clear PVC Covers, Binding Store, UK), copper tape electrodes (AT525, Advance Tapes, UK), and PVC tape insulation (AT7, Advance Tapes, UK) were cut to size. Each sheet of the ELA was prepared by attaching the copper electrodes on each side of the PVC sheet to ensure zipping from every hinge point (figure 2(a)). Each electrode was then insulated with PVC tape (black) with a maximum breakdown voltage of 8000 V. Two layers of PVC tape were used between electrodes to prevent breakdown at higher voltages. The sheets were stacked, and heat sealing was used to create the hinges that would result in a uniform lattice structure. Once the hinges were created, the flat ELA was opened and inserted into the mould for annealing in the oven.

PVC has a glass transition temperature in the approximate range between 70 °C and 100 °C [15], which is well within the ranges of standard laboratory ovens. Preliminary experiments showed that at 70 °C the PVC sheet begins to soften, but higher temperatures cause the plastic sheets to warp due to internal stresses. The ABS used to fabricate the mould has a higher glass transition temperature of approximately 105 °C. Thus, we placed each sheet of the ELA into the mould and annealed at 70 °C for sufficient time to allow the PVC to relax into the shape of the mould and to form the desired configuration. The mould was then removed from the oven and allowed to cool to room temperature. The stiff annealed PVC structure was then removed.

This process can be repeated with different dimensions to produce ELAs with smaller or larger cells, or blocks of ELAs with different dimensions. To demonstrate this, we built a basic 2D 2 × 4 cell lattice ELA, and a 3D 2 × 4 × 3 cell cuboid ELA using three electrodes on each sheet face connected in series as shown in figure 2(b).

2.2. Experimental method

Isometric testing was conducted on the 2D ELA to determine the relationship between the generated force and the voltage applied across electrodes. We investigated the effect of compression of the ELA on total contractile force. The lattice was mounted in a test rig that would limit out of plane movement but allow the lattice to expand horizontally when contracted. This horizontal freedom was achieved using long arms with pin joints attached to anchor points on the ELA, created using custom acrylic clips (see figure 3). The long arms ensure a close-to-linear transmission of force.

The bottom mount of the test rig was attached to a precision jack stand to manually control the compression of the ELA. The compression of the ELA was recorded using a laser displacement sensor (LK-G402, Keyence, Japan) by measuring the displacement of the jack surface. The top mount was attached to a load cell (DBCR-10N-002-000, Applied Measurements Ltd, UK) to record the force exerted by the ELA when a voltage was applied. Liquid dielectric in the form of silicone oil (378 356, Sigma–Aldrich, United States) was added to the hinges of the ELA using a micro pipette prior to each trial to ensure consistency between experiments. High voltage was provided by a high-voltage amplifier (10HVA24-BP1, UltraVolt, USA), driven by a multifunction I/O device (NI USB-6343, National Instruments, USA) which interfaced with a laboratory computer running MATLAB.

The resting height of the pre-formed 2D ELA was 57 mm. All measured forces were converted to stress, by dividing the measured force over the active area of the electrode (12 mm × 128 mm = 1.536 mm^2). The 2D ELA was tested at the ELA's neutral height and at heights from 20 mm to 70 mm at 10 mm intervals. This corresponds to compression values of 64.9% to −22.8%, the ratio of the height difference to the neutral height. Negative values of actuator compression indicate extension.

At each compression, voltages were applied in 1000 V intervals from 2000 V to 7000 V for 15 s at each step in an ascending staircase profile. The measurements from the last 1 s of each voltage interval were averaged to obtain the force measurement at that voltage for each trial. A total of three trials were conducted at each compression. After the application of each ascending staircase profile, the test was repeated with a descending staircase profile from 7000 V to 2000 V in 1000 V steps for each compression.

For the 3D ELA (figure 2(b)), the power required to fully contract the actuator was of particular interest, therefore voltage and current were recorded. Resonance analysis was also conducted in isotonic configuration by attaching a mass platform to the top of the actuator and applying a sinusoidal voltage profile at resonant frequency. The 3D ELA was tested with added masses of 25 g, 50 g, 75 g and 125 g. The displacement of the mass platform on the cubic actuator in each trial was recorded with the laser displacement sensor, and the results were used to calculate the mechanical power and energy characteristics of the actuator.

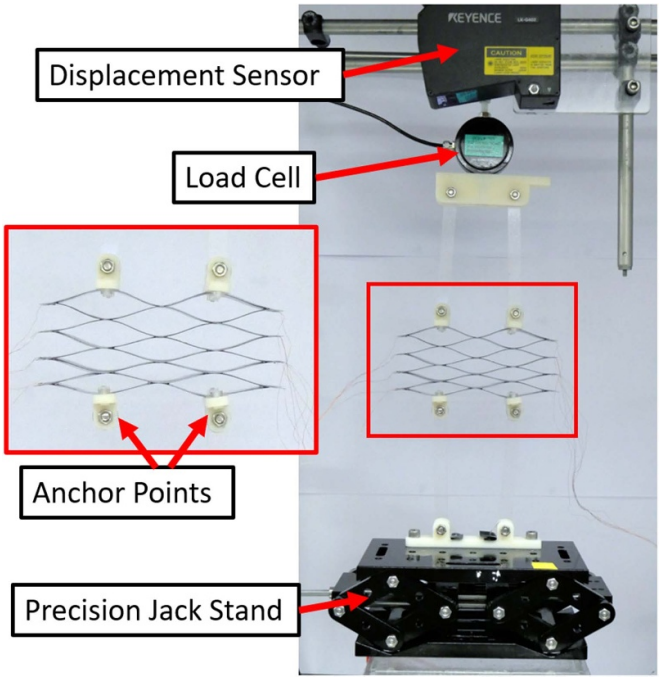

Figure 3. Experimental setup for isometric testing.

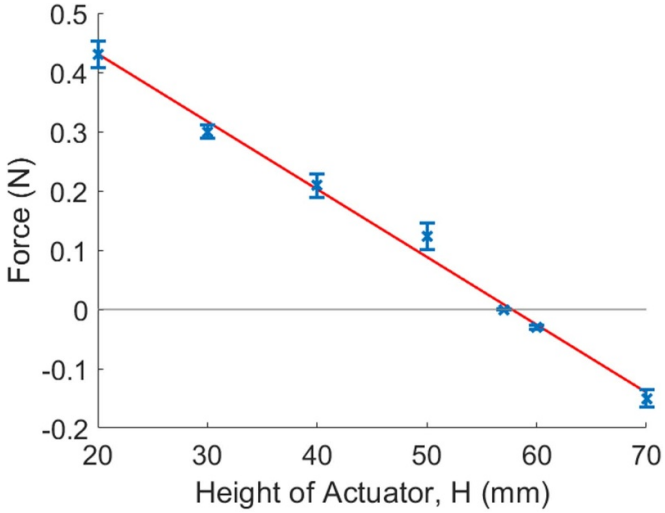

Figure 4. Force measurement against height of the 2D ELA actuator when no voltage is applied, showing the approximately linear relationship. The red line indicates a linear line of best fit according to the least-squares method, $R^2 = 0.9931$. Error bars show the mean value with ± 1 standard deviation. The equivalent spring constant is approximately 11.4 N m^{-1}.

3. Results and discussion

3.1. Isometric testing with the 2D lattice actuator

From figure 4, it can be seen that when not electrically-charged, the pre-formed structure of the 2D ELA has an almost linear passive force-displacement profile, behaving as a linear spring with a spring constant of approximately 11.4 N m^{-1}. This spring force helps the actuator return to its pre-actuated state and acts against the electrostatic contractile force exerted by the actuator.

When charged, the exerted stress increased with increasing voltage (figure 5(a)). This was due to the electrostatic forces generated which are directly proportional to the potential difference between electrodes. When the actuator is compressed (positive compression percentages in figure 5), the initial tensile stress was below zero, and the electrostatic force must first overcome the extensive spring force of the lattice structure. This was achieved at close to 3000 V for all compressions, after which the actuator exerted true tensile stress. The highest tensile stress occurred at 64.9% compression at 5000 V, with a value of approximately 184 Pa (force of 0.283 N).

Furthermore, it is observed that the slope of this relationship at close to full compression (64.9%) is steeper than at highest tested extension (-22.8%), as shown in figure 5(a). From equation (1), the strength of the exerted attractive force is inversely proportional to the distance between electrodes. Therefore, larger compression causes lower average hinge angle, which directly increases electrostatic forces. This can be seen in figure 5(a) which shows higher tensile stresses at higher compressions. It is also interesting to note that at 5000 V, the force generated at different compressions is approximately constant (see figure 5(b)), implying an equilibrium is reached between the electrostatic forces generated and the intrinsic spring forces at different compressions. This provides potential for a 'constant force' actuator which exerts the same tensile force regardless of its position, which could be useful in certain robotic, human interface and medical applications.

Figures 5(c) and (d) show the tensile stress difference between actuation and zero voltage. This gives us a clearer picture of the active stresses that are generated by the 2D ELA without the effect of the passive structural forces. From these figures, at 64.9% compression with 5000 V the ELA can generate approximately 472 Pa of pure tensile stress, or 0.727 N tensile force. This implies that a lattice actuator with a rest height at this compression could generate that amount of stress. As the actuator weighs 20 g, the maximum specific tensile stress of the 2D ELA is approximately 9.2 kPa kg^{-1} (14.13 N kg^{-1} specific force), and the specific tensile stress difference is approximately 23.67 kPa kg^{-1} (36.35 N kg^{-1} specific force). To find the force density of the lattice actuator, we divide the tensile force measured by the volume of the actuator. The dimensions of the 2D ELA give a volume of approximately 2.73×10^{-4} m^3, and a force density of 1.04 kN m^{-3}, or a force difference density of 2.66 kN m^{-3}.

Although trials were run with voltages up to 7000 V, the device behaviour became non-uniform at voltages above 5000 V. At higher voltages, the cells did not close at the same rate, which affected repeatability; this phenomenon is illustrated in figure 6(a). At 2000 V the contracted cells are approximately the same size, but at 7000 V some cells started closing while others stayed open. Like many other electrostatic actuators, ELAs are prone to pull-in instability, i.e. once they reach a certain voltage that initiates zipping, they will continue

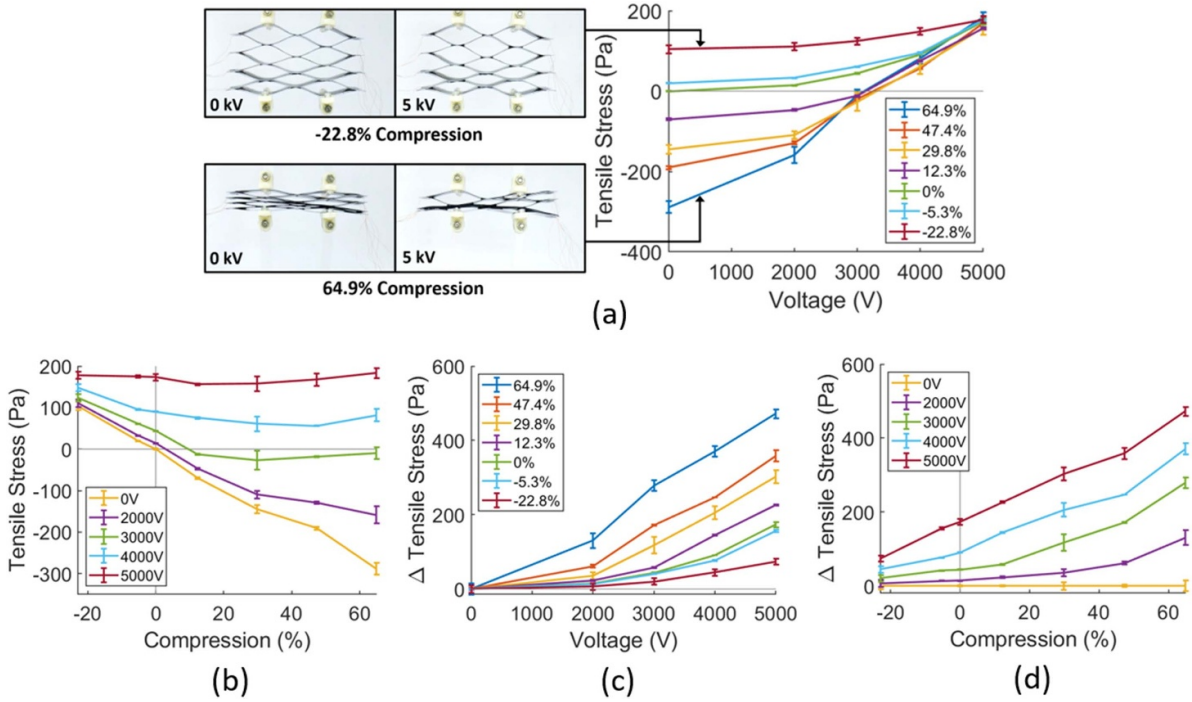

Figure 5. Results of isometric testing for ascending voltage trials. (a) Tensile stress versus applied voltage at different compressions (shown as percentage). The inset photos show the shape of the lattice actuator while actuated at a voltage of 0 and 5 kV at different compressions. (b) Tensile stress versus compression at different voltages. (c), (d) The relationship between tensile stress difference and (c) voltage or (d) compression.

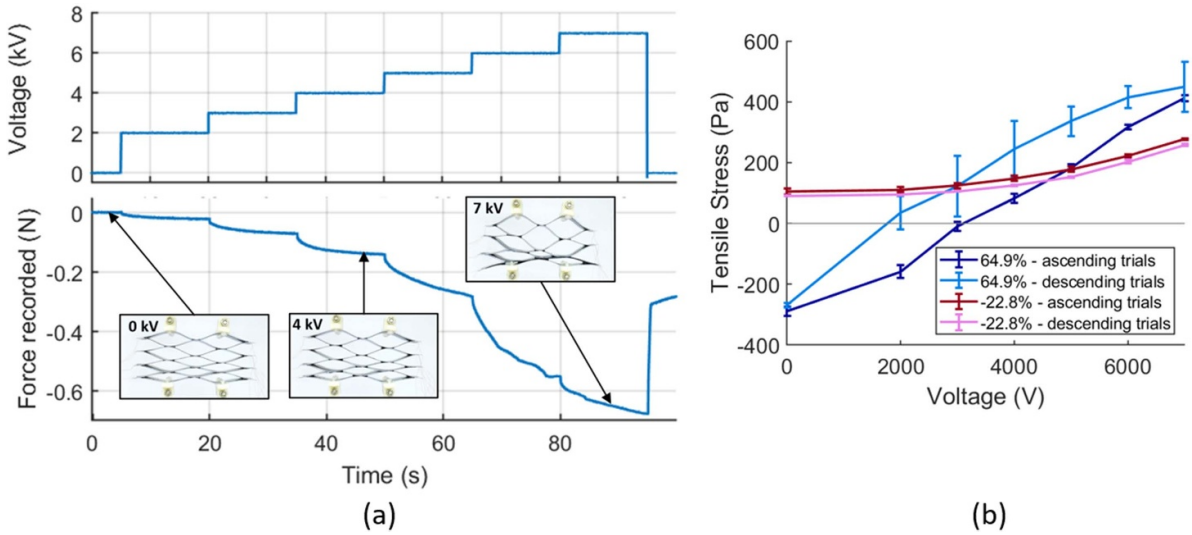

Figure 6. (a) Force measurement at neutral height when applying an ascending staircase voltage profile. The negative measurements correspond to tensile force. The measured force starts to become unstable at 6000 V. (b) The difference of measured tensile stress between ascending and descending voltage trials at two different compressions.

zipping until the actuator is closed. As a smaller hinge angle makes it easier to start zipping, this means that zipping actuation will be biased towards cells that are more closed when at rest. This includes the cells at the bottom of the ELA which are compressed by the weight of the cells above it. In addition, the inter-connected nature of the lattice structure means that closing cells will cause other cells to open. This may result in further nonlinear and unpredictable behaviour.

The observed effect of gravity on the compliant structure appears to place limitations on how large the actuator can be scaled. Varying the size of the cells and using materials with different stiffness and weight may allow larger structures to be built while still ensuring a uniform cell size when oriented vertically. Although horizontal mounting of the actuator may reduce the compression of the cells in the lower rows, we observed that it does not necessarily result in more

even actuation. A more thorough way to tackle the issue of uneven zipping is to implement methods of controlling the voltages applied to each cell to ensure that they close uniformly. This can be achieved by using closed-loop control together with the self-sensing capability of the ERAs [11, 12].

As each cell of the actuator behaves as a spring, it is expected that increasing the number of cells in parallel or in series will result in the same changes in spring constant as with parallel and series springs, respectively. Accordingly, we expect that a decrease in the number of cells in series will reduce the actuation stroke and a decrease in parallel cells to result in a decrease in actuation force. This is supported by the observations recorded by Taghavi *et al* with ERAs in series and parallel configurations [8]. However, due to the inherent compliance of the structure and dependence on the hinge angle, the relationship may not be linear. Further investigation into the effects of scaling the lattice structure and varying the parameters of the cells would be of great value to identify the design parameters that would allow this equilibrium between spring forces and electrostatic forces to be tuned. In figure 6(b), it is observed that at higher compressions, there is a significant difference in the tensile stresses recorded in the ascending and descending voltage trials. At 64.9% compression, the tensile stresses in ascending voltage trials at the steps 2000–6000 V were much lower than the tensile stresses in the corresponding descending voltage trials. The difference is attributed to the cohesive forces exerted by the liquid dielectric when the cells are closed, which increases the time needed to relax to their original shape. At 64.9% compression, the cells were almost closed, so the opposite surfaces of the cell zip together fully when actuated (see figure 5(a)). At −22.8% compression, the cells were held open and do not zip fully closed, so cohesive forces do not affect the actuator behaviour. The larger error bars at 64.9% compression support this observation. The measurements taken with a descending staircase voltage have higher standard deviation due to the unpredictable nature of the relaxation of the lattice when the voltage is decreased. In comparison, the measurements with an ascending staircase voltage at 64.9% compression have a lower standard deviation as the cells close with each step in increasing voltage and the cohesive forces do not interfere with the action.

For applications which require a more responsive and repeatable actuator, the use of a material with functionalised surface properties may help with rapid de-electroadhesion of the electro-lattice layers, or a lower charging time [16]. The lattice structure can also be constructed with a stopper within the cells to prevent full zipping, using a dielectric liquid with lower viscosity [8], or with an additional integrated actuator to generate out-of-plane vibrations to encourage rapid release [17].

3.2. Isotonic testing with the cube actuator

For the 3D ELA, we demonstrated that it could compress itself from approximately 54 mm to 4 mm (close to its constituent material thickness); a compression of 92.6% over the course of 2.6 s (figure 1 and supplementary video S1 (available online at stacks.iop.org/SMS/30/125034/mmedia)). When a decreasing ramp voltage, starting at 10 000 V and down to 5000 V within a period of 5 s, was used, the average contraction rate was 35.6% s^{-1}. The decreasing ramp voltage was required due to the current limitations of the high-voltage amplifier which was approximately 150 μA. Once fully contracted, a voltage as low as 5000 V was sufficient to keep it closed (this self-locking mechanism has been explored in [10]). The electrical power measured at this point was approximately 0.44 W to hold this contracted position. Once the voltage was removed, it slowly returned to its original height due to the internal spring force of the structure. After 5 s without applied voltage, it recovered approximately 45% of its height, and it regained approximately 91% of original height after 20 s (figure 7(a)). The speed of relaxation can be increased using methods to accelerate de-electroadhesion (as above).

The high voltages required to actuate the ELA to full contraction may be undesirable in some applications such as wearables. In addition, high voltages increase the chance of electrical breakdown of the ELA, which can result in arcing and permanent failure, so it is preferable to reduce the working voltage. According to equation (1), a thinner and higher permittivity insulator or a lattice with a smaller average hinge angle (e.g. smaller cells) which provide smaller distances between electrodes can potentially reduce the working voltage. For example, as shown in figure 5(c), moving through the range of compressions with decreasing average hinge angle results in an increase of up to 150 Pa in tensile stress at 2000 V. Aside from electrical breakdown, repeated contraction of the ELA may also cause plastic deformation of the PVC sheets, preventing the ELA from fully returning to its original height. These issues can also be addressed by exploration of other manufacturing methods and materials.

Stroke mechanical power was calculated as the change in gravitational potential energy with stroke on the cube actuator, $mg\,(\Delta H)$, where m, g and ΔH are a loaded mass at the top of the actuator, gravitational acceleration, and actuation stroke, respectively. The highest stroke mechanical energy of approximately 0.005 J was achieved with a mass of 125 g oscillating at 5.2 Hz through an amplitude of approximately 4.1 mm. Since the mass of the cube actuator was 56.5 g, specific energy is 0.09 J kg^{-1}. The power of the cube actuator was calculated as the sum of the derivatives of the potential energy and kinetic energy, $\frac{\mathrm{d}}{\mathrm{d}t}\,(mgh) + \frac{\mathrm{d}}{\mathrm{d}t}\left(\frac{1}{2}mv^2\right)$. The highest power was measured in the same trial, where it achieved a maximum power of 0.090 W and average power of 0.048 W (see figure 7(b)), implying a peak specific power of 1.59 W kg^{-1} and average specific power of 0.85 W kg^{-1}. Power density was calculated as power divided by cube actuator volume. With an actuator volume of 7.34×10^{-4} m^3, this implies a maximum power density of 1.22 kW m^{-3} and an average power density of 0.66 kW m^{-3}. The energy density of the cube was calculated in a similar way using stroke mechanical energy in place of power, giving 6.81 J m^{-3}.

The efficiency of the ELA was calculated from the average mechanical power and average electrical power obtained from the product of the recorded voltage and current during

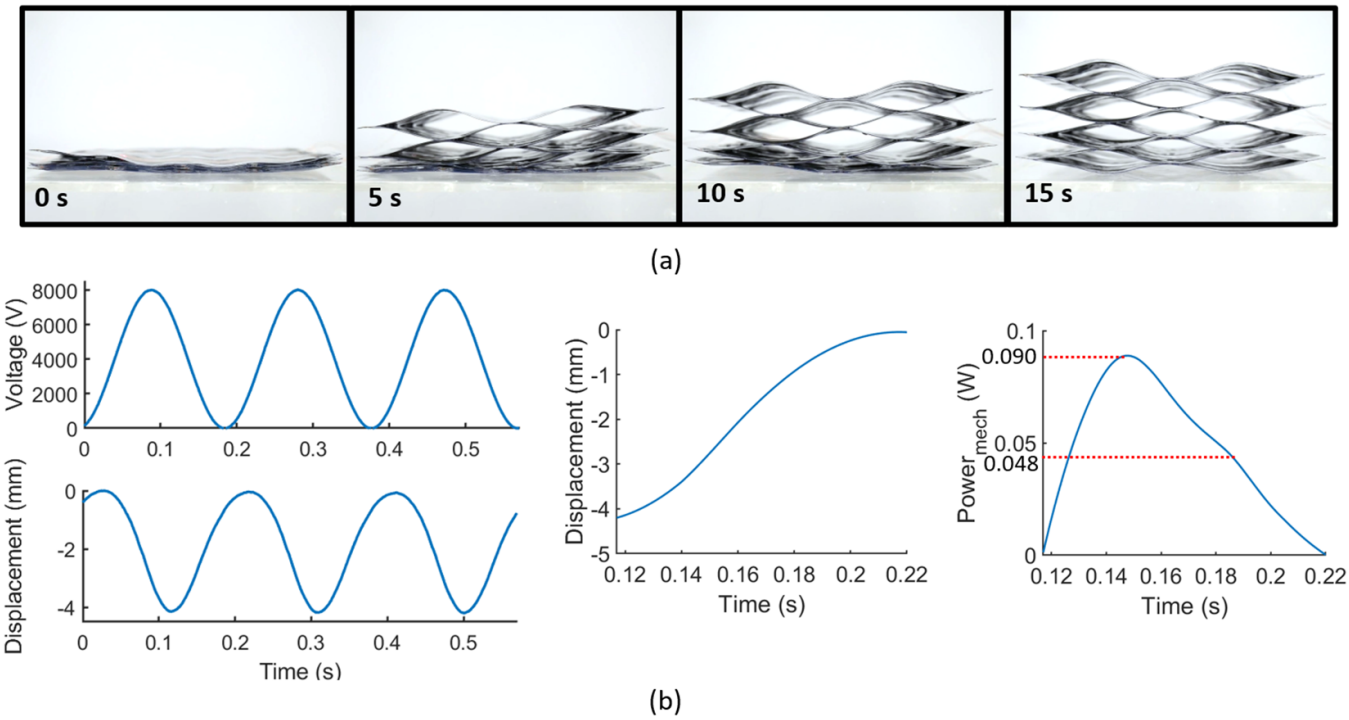

Figure 7. (a) Photos showing the relaxation of the 3D ELA after removing the potential difference in full contraction tests. (b) Mechanical power output testing using a sinusoidal input voltage at resonance. To the right, the mechanical power output upon contraction of the actuator is illustrated, showing a peak power of 0.090 W and an average power of 0.048 W.

the experiment, which gave a value of approximately 17.3%. Leakage current accounts for some of the losses experienced by the ELA, as well as mechanical energy lost due to the viscoelasticity of the structure.

4. Conclusion

In this paper we have demonstrated the manufacture of a novel active ELA structure exploiting the electrostatic ribbon actuation phenomenon and have characterised its behaviour. By using a thermoplastic backing material that can be easily preformed into the required shape, we constructed an ELA that could exert a maximum tensile stress of 184 Pa. The resulting structure also exhibited spring-like behaviour which interacts with the electrostatic forces generated upon activation, giving rise to a potentially tuneable compliant actuator. The maximum tensile stress variation between 0 and 5000 V was 472 Pa. At higher voltages, pull-in instability of the ELA caused non-uniform actuation of the cells in the lattice. Future development aims to address this problem using the self-sensing capability and controllability of electrostatic ribbon actuation to control each cell of the lattice. Further work includes manufacturing lattices with cells of different dimensions to understand how this might affect the properties of the lattice structure.

We then expanded the lattice actuator to make a cuboid-shaped ELA with a height of 54 mm before actuation and which fully contracted down to 4 mm upon activation with a decreasing ramp voltage. It achieved full contraction after 2.6 s, implying a contraction rate of approximately 35.6% s^{-1}, reaching a contraction of 92.6%. The actuator returned to approximately 91% of its original height after 20 s. This could be improved by introducing stoppers between the layers to prevent full zipping, modifying surface properties, or using less viscous dielectric liquids. The 3D cuboid ELA was able to remain at 92.6% contraction with a power consumption of 0.44 W. This ability to contract itself to extremely low thickness of 4 mm and maintain its contraction in a low power state has promising applications for storage of folding structures or robots for remote deployment. Further experiments will be conducted to study the effect of long-term contraction and storage of the actuator on its performance.

Data availability statement

The data that support the findings of this study are openly available at the following URL/DOI: 10.5523/bris.n08fth26gqjn2txmgx2e04q75.

Acknowledgments

S H was supported by the Royal Society—ERA Foundation Translation Award TA\R1\170060. T H was supported by the Royal Academy of Engineering and the Office of the Chief Science Adviser for National Security under the UK Intelligence Community Postdoctoral Fellowship Programme. R S D was supported by the Engineering and Physical Sciences Research Council (EPSRC)

through Grants EP/L015293/1 and EP/S026096/1. M T was supported by EPSRC Grant EP/R02961X/1. J R was supported by EPSRC Grants EP/L015293/1, EP/M020460/1, EP/R02961X/1, and EP/S026096/1; the Royal Academy of Engineering through the Chair in Emerging Technologies scheme; and Royal Society—ERA Foundation Translation Award TA\R1\170060.

ORCID iDs

Sam Hoh https://orcid.org/0000-0002-9808-8789
Tim Helps https://orcid.org/0000-0001-5122-8257
Richard Suphapol Diteesawat https://orcid.org/0000-0001-7002-5658

References

[1] Rus D and Tolley M T 2015 *Nature* **521** 467–75
[2] Laschi C, Mazzolai B and Cianchetti M 2016 *Sci. Robot.* **1** eaah3690
[3] Hines L, Petersen K, Lum G Z and Sitti M 2017 *Adv. Mater.* **29** 1603483
[4] Legtenberg R, Groeneveld A W and Elwenspoek M 1996 *J. Micromech. Microeng.* **6** 320
[5] Holger C, Schenk H, Kaiser B, Langa S, Gaudet M, Schimmanz K, Stolz M and Lenz M 2015 *Nat. Commun.* **6** 10078
[6] Samatham R *et al* 2007 Active polymers: an overview *Electroactive Polymers for Robotic Applications: Artificial Muscles and Sensors* ed K J Kim (Berlin: Springer) pp 1–36
[7] Acome E, Mitchell S K, Morrissey T G, Emmett M B, Benjamin C, King M, Radakovitz M and Keplinger C 2018 *Science* **359** 61–65
[8] Taghavi M, Helps T and Rossiter J 2018 *Sci. Robot.* **3** eaau9795
[9] Suo Z 2010 *Acta Mech. Solida Sin.* **23** 549–78
[10] Taghavi M, Helps T and Rossiter J 2020 *IEEE Int. Conf. on Robotics and Automation (ICRA)* (https://doi.org/10.1109/icra40945.2020.9196849)
[11] Bluett S, Helps T, Taghavi M and Rossiter J 2020 *IEEE Robot. Autom. Lett.* **5** 3931–6
[12] Diteesawat R S, Fishman A, Helps T, Taghavi M and Rossiter J 2020 *Front. Robot. AI* **7** 144
[13] Diteesawat R S, Helps T, Taghavi M and Rossiter J 2021 *Sci. Robot.* **6** eabc3721
[14] Qiu J, Lang J H and Slocum A H 2004 *J. Microelectromech. Syst.* **13** 137–46
[15] Reding F P, Walter E R and Welch F J 1962 *J. Polym. Sci.* **56** 225–31
[16] Cao C, Gao X, Guo J and Conn A 2019 *Appl. Sci.* **9** 2796
[17] Gao X, Cao C, Guo J and Conn A 2018 *Adv. Mater. Technol.* **4** 1800378